Journal of Materials Chemistry C

Accepted Manuscript

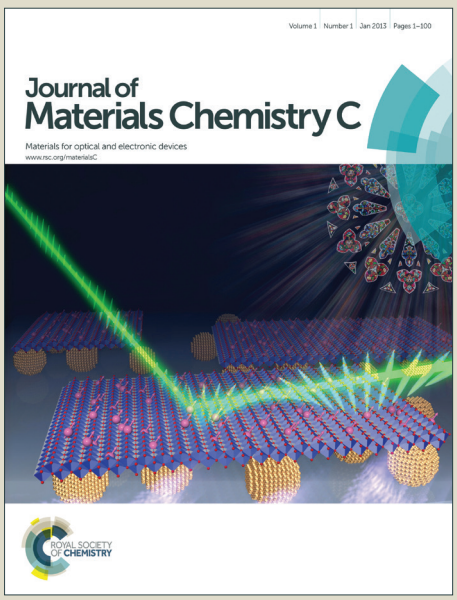

ROYAL SOCIETY OF CHEMISTRY

www.rsc.org/materialsC

Journal of Materials Chemistry C RSCPublishing

COMMUNICATION

High-Yield Synthesis of Gold Nanoribbons by Using Binary Surfactants

Cite this: DOI: 10.1039/x0xx00000x

Yong Xu,[a,†] Xuchun Wang,[a,†] Lei Chen,[a] Yang Zhao,[a] Liu He,[a,b] Peipei Yang,[a] Haihua Wu,[a] Feng Bao,[a] and Qiao Zhang*[,a]

Received 00th November 2014,
Accepted 00th December 2014

DOI: 10.1039/x0xx00000x

www.rsc.org/

In this Communication, we report a seeded growth protocol for the synthesis of gold nanoribbons with high morphological yield by using a binary surfactant system. The detailed formation process and the potential SERS application of gold nanoribbons have been systematically investigated.

Nanoribbons (also named as nanobelts), defined as ribbon- or belt-like nanostructures with thin thickness, have drawn much attention since the seminal report on ZnO nanoribbons by Wang *et al* in 2001.[1] It has been considered as an ideal system for fully understanding the dimensionally confined transport phenomena because nanoribbons can be regarded as an intermediate morphology between one-dimensional (e.g., nanowires, nanorods) and two-dimensional (e.g., nanoprisms, nanoplates) nanostructures. Additionally, research on its growth mechanism may shed some light on the growth mechanism of anisotropic nanostructures.[2] As a result, much effort has been devoted to the synthesis of nanoribbons with controlled composition, length, properties, etc.[3,4]

Research on gold nanostructures has become a hot topic due to their shape-dependent optoelectronic and physiochemical properties, as well as the potential applications in diverse fields, such as biomedicine,[5,6] sensing,[6,7] surface-enhanced Raman scattering (SERS),[8,9] photothermal therapy,[10,11] catalysis[12-17] *etc*. With the advanced nanotechnology, one can utilize colloidal protocols to make various shaped gold nanostructures, including nanorods,[18,19] nanoplates,[20-22] nanocubes,[23,24] and nanobipyramids.[25,26] However, there are only a few protocols that can produce gold nanoribbons. For example, Han *et al*. have successfully synthesized ultra-thin gold nanoribbons with an average thickness of 10 nm by a sonochemical route in the presence α-D-glucose. The obtained gold nanoribbons are single crystalline with preferential growth along the Au [111] direction.[27] Zhang *et al*. reported the synthesis of gold nanoribbons via a self-assembly of triangular gold nanoplates using poly(vinyl)pyrrolidone (PVP) as the capping agent. Zhao and co-workers synthesized gold nanobelts in an aqueous mixed surfactant solution containing CTAB and the anionic surfactant sodium dodecylsulfonate (SDSn). It is found that the final structure of gold nanobelts is determined by the reaction temperature.[28] The Hassel group prepared single crystalline gold nanoribbon arrays with different lengths via a combined method consisting of directional solid-state transformation of a Fe-Au eutectoid and a selective phase dissolution of Fe.[29,30] Although impressive progress has been achieved, some challenges still remain, including lack of clear formation mechanism, low-volume production, and high cost, which have seriously impeded its practical applications.

Seeded growth method has proven to be a powerful colloidal approach for the synthesis of anisotropic gold nanostructures since the seminal report on the synthesis of gold nanorods by Murphy et al in the year of 2001. Recently, it has been pointed out that the pre-reduction of Au^{3+} to Au^{+} by using a weak reducing agent (such as aromatic additives and unsaturated fatty acid) can significantly improve the quality of obtained gold nanostructures in the seeded growth approach.[18,19,31,32] For example, Ye and co-workers shows that the additives can help to improve the quality of gold nanorods and reduce the required concentration of CTAB.[31] In another account from Ye *et al*, a significant improvement in the dimensional tunability and monodispersity of gold nanorods has been achieved via the seeded growth method by using CTAB and sodium oleate (NaOL) as the binary surfactant.[18] Although the detailed functions of the binary surfactants were not mentioned, this work indeed provided us the necessary insight into the morphology-controllable synthesis of nanostructures by using binary surfactants or other additives.

In this work, we report the synthesis of gold nanoribbons through a convenient seeded growth approach utilizing a binary surfactant system containing CTAB and NaOL. To our best knowledge, this is the first report on the synthesis of gold nanoribbons through a seeded growth method. By varying the reaction parameters, such as reaction time and reagent concentration, gold nanoribbons with tunable length and high yield can be obtained. A systematic study has been carried out to investigate the growth mechanism of gold nanoribbons. It is found that NaOL may have dual functions in the growth process: it can not only act as a weak reducing agent that can pre-reduce Au^{3+} to Au^{+}, but also can act as a negatively charged surfactant that can reduce the required concentration of CTAB. As a result, gold nanoribbons with high morphological yield (>90%) can

be obtained when the concentration of CTAB is only 10 mM, which is much lower than the literature reports.

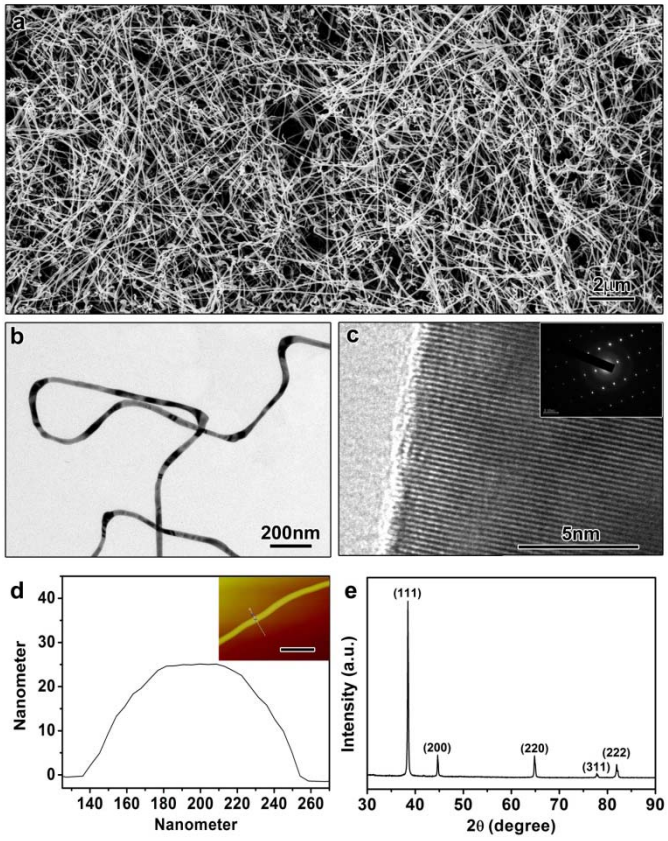

Figure 1 Typical SEM image (**a**) and TEM image (**b**) of the gold nanoribbons; (**c**) High-resolution TEM (HRTEM) image of gold nanoribbon; the inset shows the corresponding selected area electron diffraction (SAED) pattern; (**d**) The height profile of a gold nanoribbon; (**e**) XRD pattern of the gold nanoribbons. The scale bar of the inset AFM image is 500 nm.

In a typical experiment, gold seeds with size around 2-3 nm were first prepared through a rapid reduction of $HAuCl_4$ by $NaBH_4$ in the presence of CTAB. To prepare the growth solution, $HAuCl_4$ was mixed with CTAB and NaOL. The growth solution was kept at 35 ^oC for 15 min until the yellowish solution became colorless, indicating the reduction of Au^{3+} to Au^+. Certain amount of ascorbic acid was then added, followed by the addition of gold seed. The colorless solution gradually turned to reddish and brownish, suggesting the growth of gold nanostructures. The as-obtained product is gold nanoribbon with high morphological yield, as shown in **Figure 1**. **Figure 1a** shows a typical SEM image of the product, from which one can see the majority of the product are nanoribbons with length up to several tens of micrometer. TEM image shows the flexible nature of the as-obtained nanoribbons (**Figure 1b**), which can be bent over 90^o without breaking. The width of nanoribbon is around 42 nm. AFM study shows that the as-prepared gold nanoribbons have a smooth surface with the thickness around 23.9 nm (**Figure 1d**). High-resolution TEM (HRTEM) image (**Figure 1c**) shows that the lattice distance is about 0.237 nm, which is in good agreement with bulk Au (111) spacing of 0.236 nm. The selected area electronic diffraction (SAED) pattern, obtained by focusing the electron beam on a nanoribbon lying flat on the TEM grid, further proves that the nanoribbons are single crystalline with preferential growth along the Au <110> direction (inset in Figure 1c). More SAED patterns have been obtained over the entire nanoribbon and the results are essentially identical, further confirming the structurally uniform nature of the obtained nanoribbon. Powder X-ray diffraction (XRD) pattern also proves the phase structure of the gold nanoribbons. As shown in **Figure 1e**, all the diffraction peaks can be perfectly assigned to the pure crystalline face-centered cubic (fcc) gold (JCPDS card No. 04-0784).

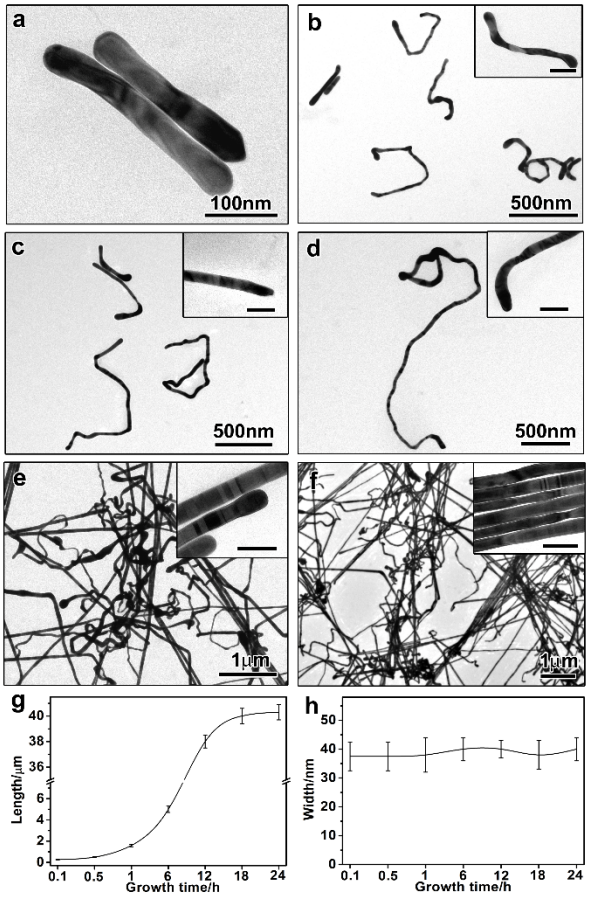

Figure 2 TEM images of product obtained at different time intervals: (**a**) 6 min; (**b**) 30 min; (**c**) 1 h; (**d**) 6 h; (**e**) 12 h; and (**f**) 18 h. (g, h) the change of length (g) and width (h) of the product as a function of the growth time. [CTAB] = 15 mM, [NaOL] = 3.8 mM, [ascorbic acid] = 9 mM, and the volume of seed is 20 μL. The scale bars in the inset TEM images are 100 nm.

To investigate the growth mechanism of gold nanoribbons, a systematic study has been carried out. We first studied the growth process carefully by monitoring the growth process through TEM measurements. **Figure 2** shows the time-dependent TEM images from the products obtained at different time intervals. Short ribbon-like nanostructures formed at the very beginning. As shown in **Figure 2a**, nanoribbons with length around 270 nm and width around 38 nm can be observed after 6 min. With the reaction continued, the length of gold nanoribbons grew gradually. When the reaction time was prolonged to 30 min, the average length of gold nanoribbons increased to 0.9 μm (**Figure 2b**). The average length of gold nanoribbons can be further increased to 1.6 μm (**Figure 2c**), 5 μm (**Figure 2d**), and 38 μm (**Figure 2e**) when the reaction time was further prolonged to 1 hours, 6 hours, and 12 hours, respectively. As plotted in Figure 2g, there is a sharp increase in the length when then

reaction time is between 1 hour and 12 hours. The growth rate reaches a platform when the reaction time is extended to 18 hours. The final length is around 40 μm (**Figure 2f**). No further length increase can be observed when the reaction time is prolonged to 24 hours, suggesting the completion of reaction. It is worth noting that although the length of gold nanoribbons increases significantly with the prolonged growth time, the width didn't change obviously over the whole process. As plotted in **Figure 2h**, the width of gold nanoribbons in all the samples is about 40 nm, suggesting that the growth of gold nanoribbons is strictly longitudinal-oriented and the growth on the (111) facet is preferentially forbidden. The preferential growth might be attributed to the capping effect of surfactant. Alkyltrimethyl ammonium halide surfactants (CTAB, CTAC) have been widely used to synthesize anisotropic gold nanostructures as they can preferentially bind to certain gold facets and protect nanoparticles from aggregation. Ye et al recently pointed out that the addition of a negatively charged additive can help to reduce the required amount of CTAB. In this system, we found that gold nanoribbons can be obtained when the concentration of CTAB is only 7.5 mM (**Figure S1**), which is much lower than that in the literature report. The optimum concentration is around 10-20 mM. In this context, we fixed the concentration of CTAB at 15 mM.

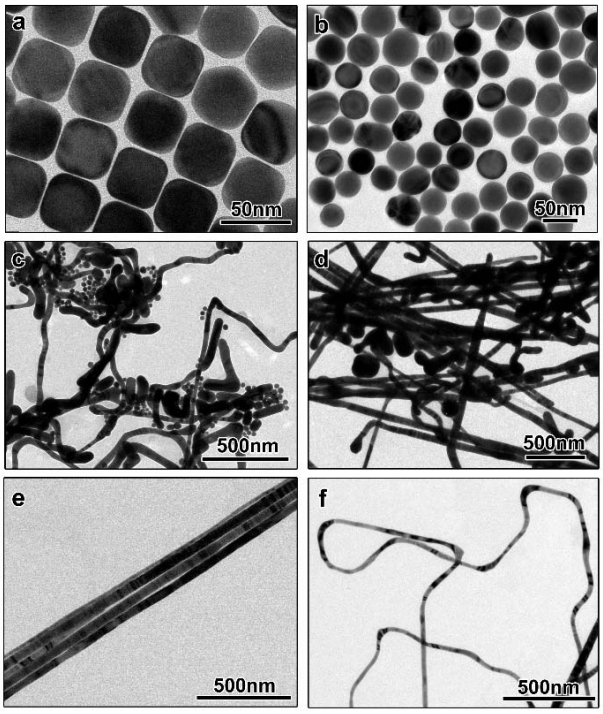

Figure 3. Effects of NaOL on the gold nanoribbons synthesis. TEM images of gold nanoribbons obtained at different concentration of NaOL: [NaOL] = (**a**) 0 mM; (**b**) 1.25 mM; (**c**) 2.5 mM; (**d**) 3 mM; (**e**) 3.8 mM; and (**f**) 8 mM. The other conditions were kept identical: [CTAB] = 15 mM, [ascorbic acid] = 9 mM, the volume of seed is 20 μL, and the growth time is fixed at 18 hours.

Since NaOL seems to be a critical factor in the synthesis of gold nanoribbons, a systematic study has been carried out to figure out the effect of NaOL. When the other reaction conditions were kept identical, the concentration of NaOL has been gradually varied. In the absence of NaOL, a reddish solution can be obtained, which is consistent with previous report.[24] TEM characterization shows that only uniform gold nanocubes can be observed, as shown in Figure 3a. The average edge length of the obtained gold nanocubes is around 40 nm. When the concentration of NaOL is 1.25 mM, the shape of the obtained gold nanoparticles evolves from cubic to spherical (**Figure 3b**), indicating that the final morphologies of the obtained nanoparticles are strongly affected by the added NaOL. When the concentration of NaOL is further increased to 2.5 mM, the formation of gold ribbons is observed, although there are still a large number of spherical nanoparticles (**Figure 3c**). The percentage of spherical nanoparticles decreases dramatically as the concentration of NaOL further increases to 3 mM, and gold nanoribbons become the dominant structure in the final products (**Figure 3d**). Further increasing the concentration of NaOL to 3.8 mM, only uniform gold nanoribbons can be observed (**Figure 3e**). The above results demonstrate that the introduction of NaOL is critical to the seeded growth of gold nanoribbons. In addition, no obvious changes in terms of the length and morphology yield are observed when further increasing the concentration of NaOL to 8 mM, indicating that the essential concentration of NaOL is as low as 3.8 mM (**Figure 3f**).

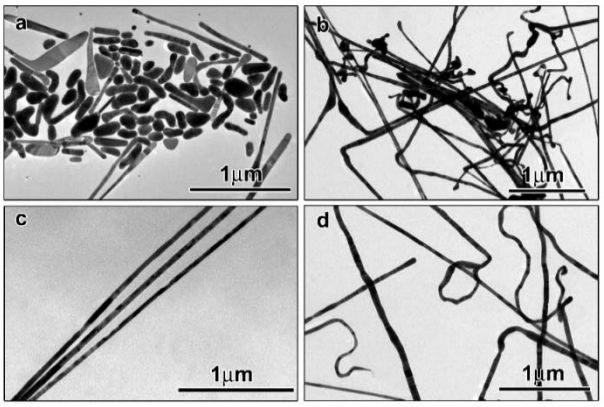

Figure 4. Effects of seed concentration on the gold nanoribbons synthesis. (a-d) TEM images of product obtained with different amount of seed solution: (**a**) 5 μL; (**b**) 10 μL; (**c**) 20 μL; (**d**) 40 μL. For all the synthesis, [CTAB] = 15 mM, [NaOL] = 3.8 mM, [ascorbic acid] = 9 mM, and the growth time is 18 hours.

To investigate the influence of seed structure as well as seed concentration on the growth of gold nanoribbons, some control experiments have been conducted. When CTAB-capped seeds were replaced by citrate-capped seeds, a mixture of irregular nanoparticles and some ribbons-like nanostructures can be obtained (Figure S4). The low yield of nanoribbons might be attributed to the larger size as well as the crystal structure of gold seeds. Without the addition of seed, only spherical nanoparticles can be obtained (data not shown). When 5 μL of diluted seed was injected to the growth solution, some irregular shaped nanoparticles can be observed, including spherical, flake-like particles as well as the gold nanoribbons with a maximum length of about 1 μm (**Figure 4a**). Some of the short nanoribbons have a width around 150 nm. The appearance of irregular shaped nanoparticles can be ascribed to the self-nucleation due to the lack of enough seeds. In the presence of 10 μL of seed, the majority of the product is gold nanoribbons with average width around 45 nm (**Figure 4b**). Only a few irregular nanoparticles can be observed, implying the suppression of self-nucleation. Pure gold nanoribbons can be obtained when the volume of seed solution is increased to 20 μL (**Figure 4c**). Further increasing the seed solution from 20 μL to 40 μL (**Figure 4d**) leads no significant change in the product morphology. A few shorter nanoribbons are observed, which is reasonable as more seeds are presented. The effect of seed

concentration on the growth of gold nanoribbons is quite consistent with the previous reports on the synthesis of gold nanorods and gold nanobipyramids, in which the aspect ratio of gold nanostructures decrease with the increased amount of seeds.[33,34] The present work indicates that the morphology of the obtained gold nanostructure is strongly depended on the numbers of seed. The optimum amount of seed is about 15 μL – 35 μL.

From the above mentioned information, we can propose a mechanism to account for the growth of gold nanoribbons. In the presence of NaOL, CTAB can form a micelle at a much lower concentration, which can act as a soft-template to direct the preferential growth of gold nanoribbons.[18] Before the addition of ascorbic acid, Au^{3+} can be reduced to Au^{+} by the unsaturated fatty acid, as indicated by the color change of solution from yellowish to colorless.[32] In the presence of ascorbic acid, Au^{+} can be further reduced to metallic Au^{0} in a controllable way. When certain amount of gold seed with suitable crystal structure is presented, the reduced gold atom will deposit to the surface of gold seed. Thanks to the capping effect of CTAB micelles, Au (111) facet has been stabilized and "blocked", thus facilitating the preferential growth.[28] As a result, uniform gold nanoribbons with high morphological yield can therefore be obtained in the optimum synthesis condition.

To further investigate the promising applications of the gold nanoribbons, SERS sensitivity was evaluated using R6G as the probing molecule due to its well-established vibrational features. As shown in **Figure 5a**, for the normal Raman spectrum of the R6G obtained with bare silicon substrate, it is very difficult to identify the characteristic peaks of R6G at the concentration of 10^{-4} M. When the obtained gold nanoribbons are employed as the substrate, a significant enhancement of the Raman intensity is observed. A series of peaks at the wave number of 1180, 1313, 1363, 1510, 1575, and 1650 cm^{-1} can be observed in the Raman spectrum, which can be perfectly assigned to the characteristic vibration features of carbon skeleton stretching in R6G (**Figure 5b**).[35] Furthermore, as shown in **Figure 5c-5d**, the SERS sensitivity shows a strong dependence on the concentration of R6G when the obtained gold nanoribbons are used as substrate. It is noted that the observed intensity from R6G at a concentration of 10^{-7} M with the assistance of the gold nanoribbons in Raman spectrum is much stronger than that obtained from R6G at a concentration of 10^{-4} M without the gold nanoribbons. The estimated enhancement factor (EF) determined by $EF = I_{SERS}C_0/I_0C_{SERS}$ is about $1.4*10^6$ with $C_0 = 0.1$ M, $C_{SERS} = 10^{-6}$ M, $I_{SERS}(1364\ cm^{-1}) = 23500$, and $I_0(1364\ cm^{-1}) = 1680$, suggesting a great performance of the obtained gold nanoribbons for SERS applications.

In summary, gold nanoribbons with high morphological yield have been successfully prepared through a seeded growth method by using a binary surfactant system composed of a positively charged surfactant, CTAB, and a negatively charged surfactant, NaOL. A systematic study has been carried out to study the formation mechanism. It is believed that sodium oleate (NaOL) can have dual functions in this process: it cannot only help to improve the morphological yield of gold nanoribbons by pre-reducing Au^{3+} to Au^{+} to control the reaction kinetics, but also help to reduce the required concentration of CTAB as well as the cost. By controlling the reaction parameters, the morphology, such as length and width, of gold nanoribbons can be readily tuned. Thanks to the simple setup, the synthesis can be easily scaled up, which will be very important for the practical applications of such unique nanostructures. Such a seeded growth method using binary surfactants may shed light on the synthesis and practical application of anisotropic gold nanostructures.

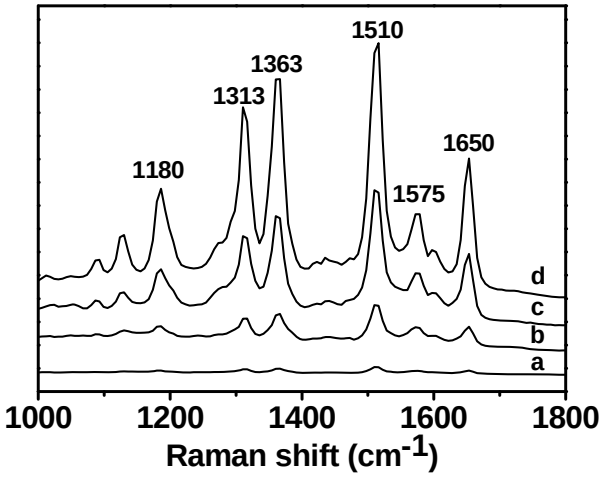

Figure 5. Raman spectra of different concentration of R6G on gold nanoribbons. (**a**) 10^{-4} M R6G without gold nanoribbons, (**b**) 10^{-7} M R6G on gold nanoribbons, (**c**) 10^{-6} M R6G on gold nanoribbons, (**d**) 10^{-5} M R6G on gold nanoribbons.

Notes and references

[a] Institute of Functional Nano and Soft Materials (FUNSOM), Soochow University, Suzhou 215123, P. R. China

[b] Department of Mechanical and Mechatronics Engineering, University of Waterloo, Waterloo, Ontario N2L 3G1, Canada.

† Y.X. and X.W. contribute equally to this paper. We thank the funding support from the National Natural Science Foundation of China (21401135), the Natural Science Foundation of Jiangsu Province (BK20140304), Jiangsu Key Laboratory for Carbon-based Functional Materials & Devices, and Collaborative Innovation Center of Suzhou Nano Science and Technology.

Electronic Supplementary Information (ESI) available: [Experimental details, additional TEM images and optical microscopy images]. See DOI:10.1039/c000000x/

1 Pan, Z. W.; Dai, Z. R.; Wang, Z. L. *Science* 2001, **291**, 1947.

2 Li, L.; Wang, Z.; Huang, T.; Xie, J.; Qi, L. *Langmuir* 2010, **26**, 12330.

3 Wang, Z. L. *Mater. Sci. Eng. Rep.* 2009, **64**, 33.

4 Terrones, M.; Botello-Mendez, A. R.; Campos-Delgado, J.; Lopez-Urias, F.; Vega-Cantu, Y. I.; Rodriguez-Macias, F. J.; Elias, A. L.; Munoz-Sandoval, E.; Cano-Marquez, A. G.; Charlier, J. C.; Terrones, H. *Nano Today* 2010, **5**, 351.

5 Hu, M.; Chen, J.; Li, Z.-Y.; Au, L.; Hartland, G. V.; Li, X.; Marquez, M.; Xia, Y. *Chem. Soc. Rev.* 2006, **35**, 1084.

6 Jain, P. K.; Huang, X.; El-Sayed, I. H.; El-Sayed, M. A. *Acc. Chem. Res.* 2008, **41**, 1578.

7 Stewart, M. E.; Anderton, C. R.; Thompson, L. B.; Maria, J.; Gray, S. K.; Rogers, J. A.; Nuzzo, R. G. *Chem. Rev.* 2008, **108**, 494.

8 Eustis, S.; El-Sayed, M. A. *Chem. Soc. Rev.* 2006, **35**, 209.

9 Kneipp, K.; Kneipp, H.; Kneipp, J. *Acc. Chem. Res.* 2006, **39**, 443.

10 Cobley, C. M.; Chen, J.; Cho, E. C.; Wang, L. V.; Xia, Y. *Chem. Soc. Rev.* 2011, **40**, 44.

11 Murphy, C. J.; Gole, A. M.; Stone, J. W.; Sisco, P. N.; Alkilany, A. M.; Goldsmith, E. C.; Baxter, S. C. *Acc. Chem. Res.* 2008, **41**, 1721.

12 Daniel, M. C.; Astruc, D. *Chem. Rev.* 2004, **104**, 293.
13 Hashmi, A. S. K.; Hutchings, G. J. *Angew. Chem. Int. Ed.* 2006, **45**, 7896.
14 Corma, A.; Garcia, H. *Chem. Soc. Rev.* 2008, **37**, 2096.
15 Hughes, M. D.; Xu, Y. J.; Jenkins, P.; McMorn, P.; Landon, P.; Enache, D. I.; Carley, A. F.; Attard, G. A.; Hutchings, G. J.; King, F.; Stitt, E. H.; Johnston, P.; Griffin, K.; Kiely, C. J. *Nature* 2005, **437**, 1132.
16 Chen, M. S.; Kumar, D.; Yi, C. W.; Goodman, D. W. *Science* 2005, **310**, 291.
17 Zhang, Q.; Lima, D. Q.; Lee, I.; Zaera, F.; Chi, M. F.; Yin, Y. D. *Angewandte Chemie-International Edition* 2011, **50**, 7088.
18 Ye, X.; Zheng, C.; Chen, J.; Gao, Y.; Murray, C. B. *Nano Lett.* 2013, **13**, 765.
19 Ye, X.; Gao, Y.; Chen, J.; Reifsnyder, D. C.; Zheng, C.; Murray, C. B. *Nano Lett.* 2013, **13**, 2163.
20 RahimáFerhan, A. *Nanoscale* 2014, **6**, 6496.
21 Beeram, S. R.; Zamborini, F. P. *Acs Nano* 2010, **4**, 3633.
22 Millstone, J. E.; Wei, W.; Jones, M. R.; Yoo, H.; Mirkin, C. A. *Nano Lett.* 2008, **8**, 2526.
23 Zhang, J.; Langille, M. R.; Personick, M. L.; Zhang, K.; Li, S.; Mirkin, C. A. *J. Am. Chem. Soc.* 2010, **132**, 14012.
24 Wu, X.; Ming, T.; Wang, X.; Wang, P.; Wang, J.; Chen, J. *ACS Nano* 2010, **4**, 113.
25 Personick, M. L.; Langille, M. R.; Zhang, J.; Harris, N.; Schatz, G. C.; Mirkin, C. A. *J. Am. Chem. Soc.* 2011, **133**, 6170.
26 Zhang, J.; Langille, M. R.; Mirkin, C. A. *J. Am. Chem. Soc.* 2010, **132**, 12502.
27 Zhang, J.; Du, J.; Han, B.; Liu, Z.; Jiang, T.; Zhang, Z. *Angew. Chem. Int. Ed.* 2006, **45**, 1116.
28 Zhao, N.; Wei, Y.; Sun, N.; Chen, Q.; Bai, J.; Zhou, L.; Qin, Y.; Li, M.; Qi, L. *Langmuir* 2008, **24**, 991.
29 Chen, Y.; Milenkovic, S.; Hassel, A. W. *Nano Lett.* 2008, **8**, 737.
30 Chen, Y.; Somsen, C.; Milenkovic, S.; Hassel, A. W. *J. Mater. Chem.* 2009, **19**, 924.
31 Ye, X. C.; Jin, L. H.; Caglayan, H.; Chen, J.; Xing, G. Z.; Zheng, C.; Doan-Nguyen, V.; Kang, Y. J.; Engheta, N.; Kagan, C. R.; Murray, C. B. *ACS Nano* 2012, **6**, 2804.
32 Scarabelli, L.; Grzelczak, M.; Liz-Marzan, L. M. *Chem Mater* 2013, **25**, 4232.
33 Vigderman, L.; Zubarev, E. R. *Chem Mater* 2013, **25**, 1450.
34 Julien, R. G. N.; Delphine, M.; Fréderic, L.; Emmanuel, C.; Jean, L.; Christophe, B.; Fréderic, C.; Alexis, M.; Michel, P.; Stephane, P. *Nanotech.* 2012, **23**, 145707.
35 Zhang, P.; Yang, S.; Wang, L.; Zhao, J.; Zhu, Z.; Liu, B.; Zhong, J.; Sun, X. *Nanotech.* 2014, **25**, 245301.

Table of Content

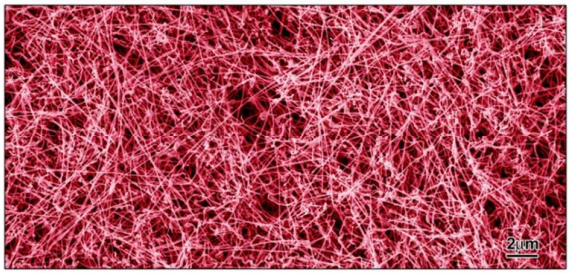

Gold nanoribbons with high morphological yield and great SERS performance have been successfully prepared by using binary surfactants.